UNDERSTANDING THE ASTROPHYSICAL-ICE NANOSTRUCTURES FORMATION THROUGH CLASSICAL MOLECULAR DYNAMICS

COMPREENDENDO A FORMAÇÃO DE NANOESTRUTURAS EM GELO ASTROFÍSICOS ATRAVÉS DA DINÂMICA MOLECULAR CLÁSSICA

Priscila Alves da Silva[1]
Sergio Pilling[2]
Rodrigo Garcia Amorim[3]

Abstract: Astrophysical ices (formed by water, among other molecules) act as a catalyst and a reservoir of carbonaceous species, both of which have major implications for astrobiology. In this work, we studied the formation of astrophysical ice nanostructures found in the interstellar medium, having a sheet of graphene as a catalyst substrate, using the classical molecular dynamics technique to model these astrophysical environments. For this, two systems were designed: the first composed of graphene and H_2O and the second composed of graphene, H_2O and CO_2. Initially, a simulation box was built where the area was delimited by graphene whose height varied from 4, 6, 8 and 10 nm. The molecules were evenly distributed throughout the box. The molecular dynamics technique proved to be a promising tool to understand the phenomenon of adsorption of molecules on the substrate, allowing us to realize that the random distribution of molecules in the system interferes with the geometric structure formed by an ice nanostructure. This study allows us to understand, from the nanometric point of view, the influence of some physical-chemical parameters, regarding the formation of nanostructures of astrophysical ices, such as the number of hydrogen bonds, the initial size of the simulation box, and its density during the freezing process.

Keywords: classical molecular dynamics; astrophysical ice; formation of substrate-adsorbed ice nanostructures; astrochemistry; astrophysics.

Resumo: Gelos astrofísicos (formados pela água, entre outras moléculas) atuam como um catalisador e um reservatório de espécies carbonáceas, ambas com grandes implicações para a astrobiologia. Neste trabalho, nós estudamos a formação de nanoestruturas de gelo astrofísico encontradas no meio interestelar, tendo uma folha de grafeno como substrato catalisador, utilizando-se a técnica de dinâmica molecular clássica para modelar esses ambientes astrofísicos. Para isso, projetou-se dois sistemas: o primeiro composto por grafeno e H_2O e o segundo composto por grafeno, H_2O e CO_2. Inicialmente construiu-se uma caixa de simulação onde a área foi delimitada pelo grafeno cuja altura variava de 4, 6, 8 e 10 nm. As moléculas foram distribuídas uniformemente por toda a caixa. A técnica de dinâmica molecular provou ser uma ferramenta promissora para entender o fenômeno da adsorção de moléculas no substrato, permitindo-nos perceber que a distribuição aleatória de moléculas no sistema interfere com a estrutura geométrica formada por uma nanoestrutura de gelo. Este estudo nos permite compreender, do ponto de vista nanométrico, a influência de alguns parâmetros físico-químicos, *no que tange a*

[1] Universidade de São Paulo - USP. E-mail: priscila_silva@usp.br.
[2] Professor pesquisador na Universidade do Vale do Paraíba – Univap. E-mail: sergiopilling@yahoo.com.br.
[3] Professor adjunto A2 na Universidade Federal Fluminense. E-mail: rgamorim@id.uff.br.

formação das nanoestruturas de gelos astrofísicos, como o número de ligações de hidrogênio, o tamanho inicial da caixa de simulação, e sua densidade durante o processo de congelamento.
Palavras-chave: dinâmica molecular clássica; gelo astrofísico; formação de nanoestruturas de gelos adsorvidas a substrato; astroquímica; astrofísica.

Identificação e disponibilidade:
(https://revista.univap.br/index.php/revistaunivap/article/view/4415, http://dx.doi.org/10.18066/revistaunivap.v29i61.4415).

1 INTRODUCTION

The interstellar medium (ISM) is the region between stars, which has temperatures ranging from 10 to 10^4 K and places where the number density of hydrogen varies roughly from 10^2-10^8 H cm^{-3} (with typical values around 1 H cm^{-3}). In addition to electromagnetic radiation, ISM matter consists of 90% molecular hydrogen, 9% helium, and the rest is distributed over heavier elements such as carbon, nitrogen, oxygen, and iron (Ehrenfreund & Charnley, 2000). Besides the gas-phase, the ISM also contains dust grains (covered or not by icy mantles) with typical dust/gas mass ratio of 1/100 (e.g. Freivogel et al., 1994; Tielens, 2005).

Organic species are observed in different regions of our universe, among which are molecular clouds, some denser regions and cold regions of the ISM (Gerakines, et al., 1999; Tielens, 2013; Van Dishoeck, 2014; Kwok, 2016; Ehrenfreund & Charnley, 2000). Understanding the physical and chemical mechanism of these regions is of great importance, because it is there that protostellar systems are formed giving rise to new planetary systems and a variety of molecules in (Ehrenfreund & Charnley, 2000). In dense molecular clouds the temperature varies from 10-30 K and the density varies from 10^4-10^8 H cm^{-3}, the cold dust grains act as chemical catalysts forming mantles of astrophysical ice, whose predominant molecular constitution is H_2O. However, we can find astrophysical ices made up of other molecules, such as CO, N_2, O_2, C_2H_2 and C_2H_4, in addition to the predominance of H_2O, which were formed from a reactive process and adsorbed to the catalyst substrate. These ices can be transported from a cold region (highly obscured) to a warmer region, changing their chemical composition and forming astrophysics ices with a greater number of atoms and a higher number of chemical bonds (Ehrenfreund & Charnley, 2000). Additionally, the astrophysical ices can be also classified as polar and nonpolar ices. Polar ice is made up of H_2O and generally evaporates around 90 K under astrophysical conditions, and thus can survive in regions of higher temperature. Nonpolar ice, on the other hand, consists of more volatile molecules with an evaporation temperature < 20 K and thus can only survive in colder regions (Ehrenfreund & Charnley, 2000).

Molecular dynamics simulations of astrophysical environments have been performed in literature by several groups with the goal to understand laboratory experiments and astronomical observations (Andersson et al., 2006; Andersson & Van Dishoeck, 2008; Anders & Urbassek, 2013; Arasa et al., 2013; Mainitz et al., 2016). Some works focused on the molecular formation or molecular destruction, other in the ice growth, and desorption processes and other focus on the chemical reaction induced by radiation of ices (Matsumoto et al., 2002; Andersson & Van Dishoeck, 2008; Zheligovskaya, 2008; Arasa et al., 2010; Arasa et al., 2013; Anders & Urbassek, 2013; Mainitz et al., 2016).

In this context, our work aims to contribute to the understanding of the formation process of polar and nonpolar astrophysical ice nanostructures, adsorbed on an electrically neutral carbonaceous substrate, using the classical molecular dynamics technique. In section 1.1 we describe the theoretical methodology in which we simulate two systems, the first composed of H_2O and the second composed of H_2O and CO_2, homogeneously distributed, representing the gas phase. Then we describe the methodology to recreate ice structure under vacuum conditions using the molecular dynamics technique, adsorbed to the catalyst substrate at a fixed temperature of 10 K. In the current simulation, to overcome the computational limitations on the integration time and the number of events, the gas number density was ~ 10^{20} molecules per cm^{-3} (low to medium vacuum domain). In spite of this value being much higher than the one found in the interstellar medium, it is still within the same molecular flow domain existent in interstellar environments. The main results and discussions are presented in section 2 and include the analysis of the formation of the astrophysical ice in different initial conditions (different pressures in the low to medium vacuum). The ice systems were characterized by considering the variation of the average distance of the molecules of the system in relation to the center of mass of graphene, the number of hydrogen bonds and the average density of the ice nanostructures. Section 3 presents the selected main conclusions of this manuscript.

2 METHODOLOGY

Computer simulations have been widely used to model phenomena already built and validated in different areas of knowledge, in addition to providing study through models in which it is difficult or impossible to obtain experimental results about a given system (Rino & Costa, 1998). The classical molecular dynamics (MD) computational technique describes the dynamic, thermodynamic and structural properties of a given system, based on the integration of Newton's equations of motion for a system of N-bodies from pre-defined initial settings.

The temporal evolution of the system is made from discrete steps as a function of time, related posteriorly to macroscopic properties through statistical mechanics, making use of the function that describes the intermolecular and intramolecular potential energy, called the force field. Classical MD enables the integration of a system involving thousands of atoms, neglecting the calculation of electronic interactions from the introduction of the concept of empirical potentials, which are analytical mathematical expressions capable of describing the interaction of two or more bodies (atoms, ions or molecules) (Rino & Costa, 1998). In addition, classical MD uses the Born-Oppenheimer approximation, that allows studying the molecular wave functions separating the nuclear displacement from electronic motion, because the temporal scale is different since the mass of the nucleus is approximately 1836 times greater than the mass of electrons. This fact leads the electron to adjust after each movement of the core over time. This approximation causes the nucleus to interact with the electrons as if they were a charged cloud, and when we analyze the electrons, they interact with the nucleus as if it was stopped, what generates the decoupling of the nucleus and electrons movement. For the application of the MD technique, we used the free software GROMACS, version 4.6.7, which makes it possible to simulate organic and inorganic molecular structures (Abraham et al., 2014). The results presented here were obtained from a high-performance computer cluster, which consists of 32 servers, with 64 Tesla k20m GPUs, 512 Intel E7-2870

Xeon processors (2.4 GHz), 4128 GB RAM and 55 TB disk, maintained by the University of São Paulo.

The force field used was AMBER-99, which can be written as the sum of intermolecular and intramolecular potentials described in the equation below (Sorin & Pande, 2005), (DePaul et al., 2010).

$$\boldsymbol{V(r) = \sum_{bonds} K_i^{bond}(r_i - r_0)^2 + \sum_{angle} K_i^{angle}(\theta_i - \theta_0)^2 + \sum_{bonds} K_i^{dihedral}[1 + cos(n_i\phi_i - \delta_i)] + \sum_i \sum_{j \neq i} 4\epsilon_{ij}\left[\left(\frac{\sigma_{ij}}{r_{ij}}\right)^{12} - \left(\frac{\sigma_{ij}}{r_{ij}}\right)^{6}\right] + \sum_i \sum_{j \neq i} \frac{q_i q_j}{4\pi\varepsilon_0 \varepsilon_r r_{ij}}} \quad [1]$$

The first term is associated with the binding or stretching potential in relation to its ideal or equilibrium value $\boldsymbol{r_0}$ and $\boldsymbol{K_i^{bond}}$ is defined as a binding constant. The second term is related to the angular strain energy in relation to an equilibrium value $\boldsymbol{\theta_0}$, where $\boldsymbol{K_i^{angle}}$ is the angular constant of this system. The third term is the associated energy due to torsion around a given chemical bond, where the constant $\boldsymbol{K_i^{dihedral}}$ consists of the value to perform the twist, $\boldsymbol{n}$ the number of maximum or minimum energy during a complete twist, $\boldsymbol{\phi}$ the dihedral angle and $\boldsymbol{\delta}$ the phase, where $\boldsymbol{\epsilon_{ij}}$ is the depth of the repulsive and attractive barrier of the potential and $\boldsymbol{\sigma_{ij}}$ is a finite distance at which the inter-particle potential is zero, $\boldsymbol{r_{ij}}$ is the distance between two atoms. For electrostatic potential $\boldsymbol{q_i}$ and $\boldsymbol{q_j}$ are the atomic charges on the atoms, $\boldsymbol{\varepsilon_0}$ is the free space permittivity constant $\boldsymbol{\varepsilon_r}$ and the relative dielectric constant of the medium.

From the force field, we can obtain the system dynamics through the Newton's motion equations, where (Abraham et al., 2014):

$$\vec{F}_i = m_i \frac{\partial^2 \vec{r}_i}{\partial t^2} \quad [2]$$

$$\vec{F}_i = -\frac{\partial V}{\partial \vec{r}_i} \quad [3]$$

where *i* is the number of particles, $\vec{F}_i$ the resultant force acting on particle i, $\boldsymbol{V}$ is the resulting potential energy for particle *i*, $\vec{r}_i$ vector position of particle i in an instant of time and $\boldsymbol{m_i}$ the mass of particle *i*. Substituting equation [1] into [3] and integrating equation [2] we obtain the position and velocity of the particles as a function of time for the desired integration period. The integration of the equations of motion was performed using the Velocity Verlet algorithm, which makes use of a small integration to describe how the trajectory of particles varies as a function of time (DePaul et al., 2010). The thermodynamic properties were studied from average parameters using statistical mechanics.

The formation of astrophysical ice nanostructures was obtained from two MD models. The first model was considered: i) system I, consisting of graphene, whose surface has dimensions of (3.812 x 3.664 nm), and H_2O and ii) system II consisting of graphene, H_2O and CO_2. Both started with the construction of a rectangular box, whose base remained fixed and consisted of a graphene structure. The volume of the box varied according to the increase in the height of the box (4, 6, 8 and 10 nm). System I was built from the insertion of 100 molecules of H_2O and system II, from the insertion of 80 molecules of H_2O and 20 molecules of CO_2. By limiting a specific number of water molecules in a box, the program groups all the H_2O molecules close

to the graphene surface. In this way, we performed approximately 80 simulations, for the two systems, for an interval of time of 1000 ps, keeping the number of particles, volume constant and adding at the end of each simulation run 100 K more than the previous temperature. This procedure was necessary for the molecules to reach homogeneity throughout the box, as can be seen in Figure 1. In this stage of the simulation, we used the Ensemble NVT with Berendsen thermostat and barostat, keeping constant the parameters: number of particles (N), volume (V) and temperature. (T) (Abraham et al., 2014). This procedure was used until the temperature of 1100 K for system I and 2800 K for system II. In the astrophysical ice formation stage, the barostat was removed from the system, which allowed the "vacuum" modeling. The thermostat used continued to be Berendsen's, and the entire system, be it for ice I or II, reaches a temperature of 10 K after a time of 100 ns.

3 RESULTS AND DISCUSSION

The results presented and discussed in the next section refer to: i) Modeling the gas phase and ii) the freeze-out phase on a cold graphene surface (ice formation). The effect of the formation of astrophysical ices adsorbed to the graphene surface will be discussed, starting from different initial configurations, the influence of the box in the approximation of the center of mass of the gas molecules in relation to the surface, the number of hydrogen bonds, both as a function of the height of the box, according to the configuration the mixture of gases in them and finally the calculation of the density from a nanometric volume of astrophysical ice.

3.1 COMPUTATIONAL MODELING OF THE GAS

The two systems built used the standard solvent of GROMACS as the water model, the SPC (Simple Point Charge) formed by 3 point charges structured in the tetrahedral form, with charge +0.41 eC for hydrogen and - 0.82 eC for oxygen and initially distributed at a temperature of 300 K and a pressure of 1 bar (Berendsen et al., 1995). Figure 1a-b shows the variation of the mass density of the system I, for the heights of 4 and 10 nm, starting from the initial temperature of 300 K until 1100 K, when the homogeneity is reached. We can observe the accumulation of H_2 O molecules close to graphene (300 K), which is also observed by a higher density in this region. The system is heated, increasing by 100 K from its final configuration, until the molecules are in a homogeneous configuration. The figure 1c-d represents the system II. Although the CO_2 molecules are randomly distributed, this does not guarantee homogeneity, which makes us repeat the heating procedure described for system I, until homogeneity is reached. In this case, there was a need for an extension in temperature so that homogeneity was achieved, as can be seen in the red graph that refers to a temperature of 2800 K. The CO_2 molecule is not explicitly presented in version 4.6.7 of GROMACS, which made us take it as version 5.0.1 by analyzing the binding parameters referring to the CO_2 molecule and thus adapting it to version 4.6.7, the oxygen charge was distributed at -0.350 eC and carbon at +0.700 eC

Figure 1 - Panels a-d show the rows confined in different boxes at temperatures of 300 K (initial) and the final temperature, which represent the homogeneous system. Homogeneity can be analyzed by mass density as a function of box volume.

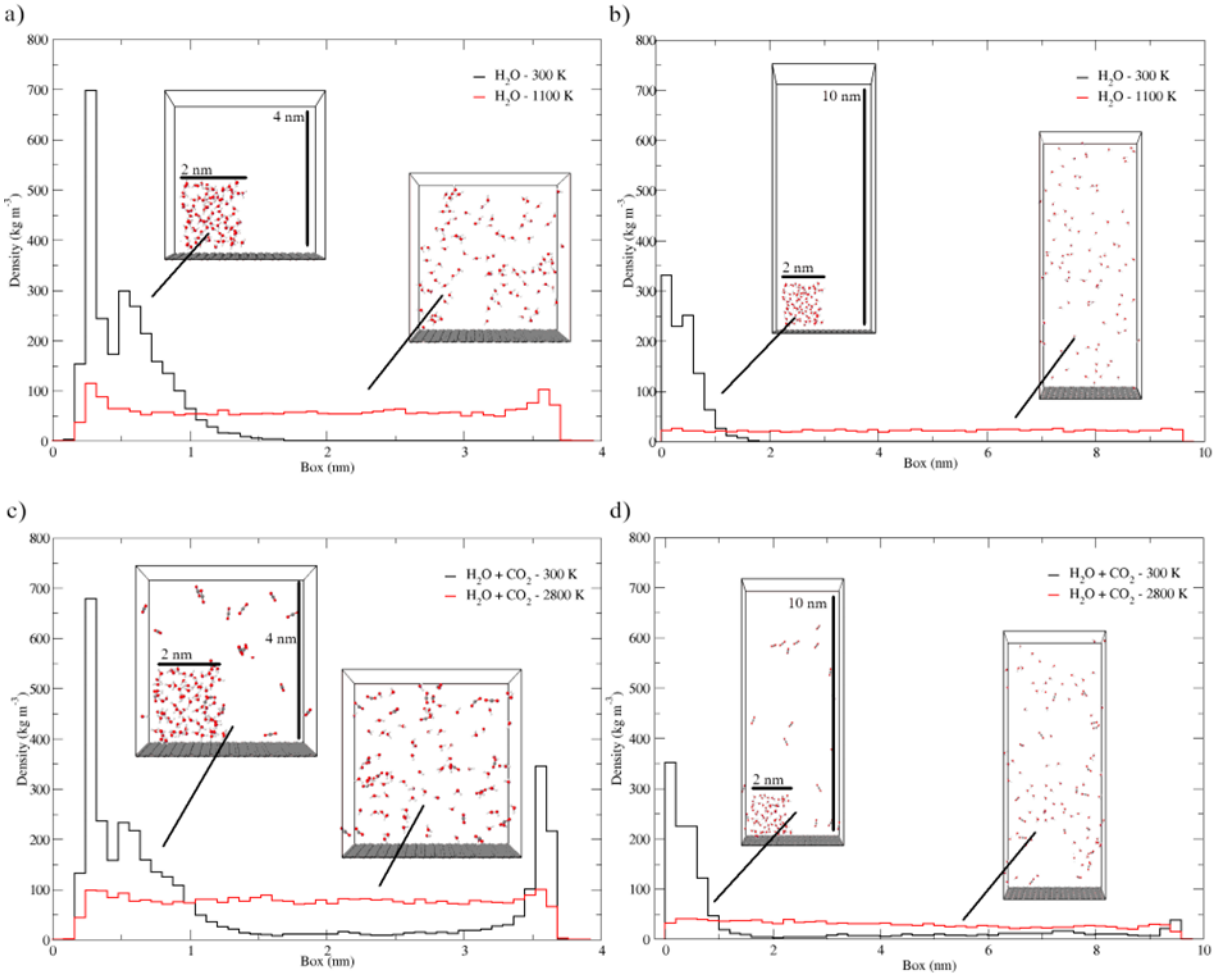

Source: Prepared by the authors.

3.2 FORMATION OF THE ASTRHOPHYSICAL ICE NANOSTRUCTURES AT 10 K

For the formation of ice adsorbed on the graphene surface, which represents a vacuum condition in molecular dynamics, we open the simulation box, which in turn confined the molecules of the system at gas phase, leaving only the graphene structure fixed at the bottom of the box. When performing this procedure, the barostat stops acting on the system, which simulates the vacuum condition in MD (Abraham et al., 2014). After obtaining the final temperature of the system, which represents an emitted distribution of emissions in the gaseous phase, we selected the last frame, represented in the panel of Figure 1a-d, to act as input for the next stage of the simulation, this one consisting of the formation of astrophysics ice at a temperature of 10 K adsorbed to the graphene catalyst substrate.

3.3 VARIATION OF THE DISTANCE FROM THE CENTER OF MASS OF THE SYSTEMS IN RELATION TO THE GRAPHENE SURFACE AS A FUNCTION OF TIME

Figure 2 shows the center of mass temporal evolution for the molecules that make up the system I and II in relation to the center of mass of the fixed graphene, during the ice formation process at a final temperature of 10 K.

Figure 2 - Panel a) movement of the center of mass of system I, in addition to the final configuration of this system forming astrophysical ice clusters, and panel b) the movement of system II, showing the final configuration of this system forming astrophysical ices, in relation to the fixed surface of graphene during the ice formation process at 10 K.

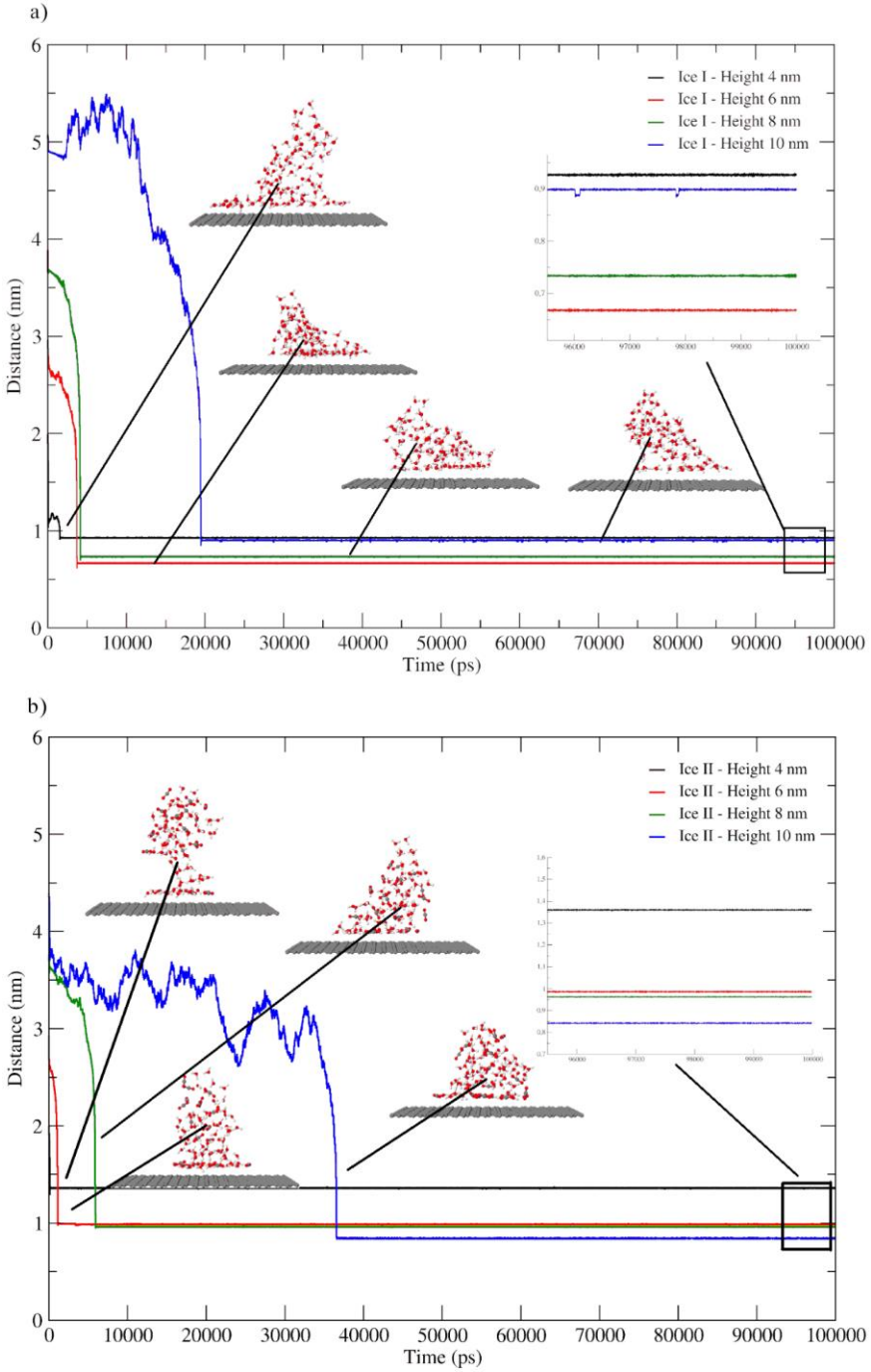

Source: Prepared by the authors.

We noticed that in both systems there was the formation of astrophysical ices adsorbed to the graphene surface. However, the average variation of the distance of the molecules that constitute each system, in relation to the graphene's center of mass and in relation to the initial height of the simulation box, differs. In system I, the molecules that were initially in a box 4 nm high, when released into a vacuum at a temperature of 10 K, reached an average height of 0.927 nm in relation to the graphene surface. The molecules that started from a 6 nm high box reached an average distance of 0.668 nm, the 8 nm system reached 0.734 nm, and the 10 nm system reached a distance of 0.899 nm, as shown in figure 3a. In general, we noticed that the average distance of the molecules that make up system II in the gas phase are further away from the center of mass of graphene when compared to system I. For the initial configuration that represents system II in a box of 4 nm in height, the average distance was 1.360 nm, for a box with the initial height of 6 nm the average distance was 0.986 nm, for 8 nm the distance was 0.962 nm and for the height of 10 nm the average distance was 0.842 nm, as we can see in figure 3b.

Figure 3 - Shows the average distance of the center of mass of the molecules of system I and II in relation to the graphene surface in relation to the initial height of the simulation box, forming ice I and II.

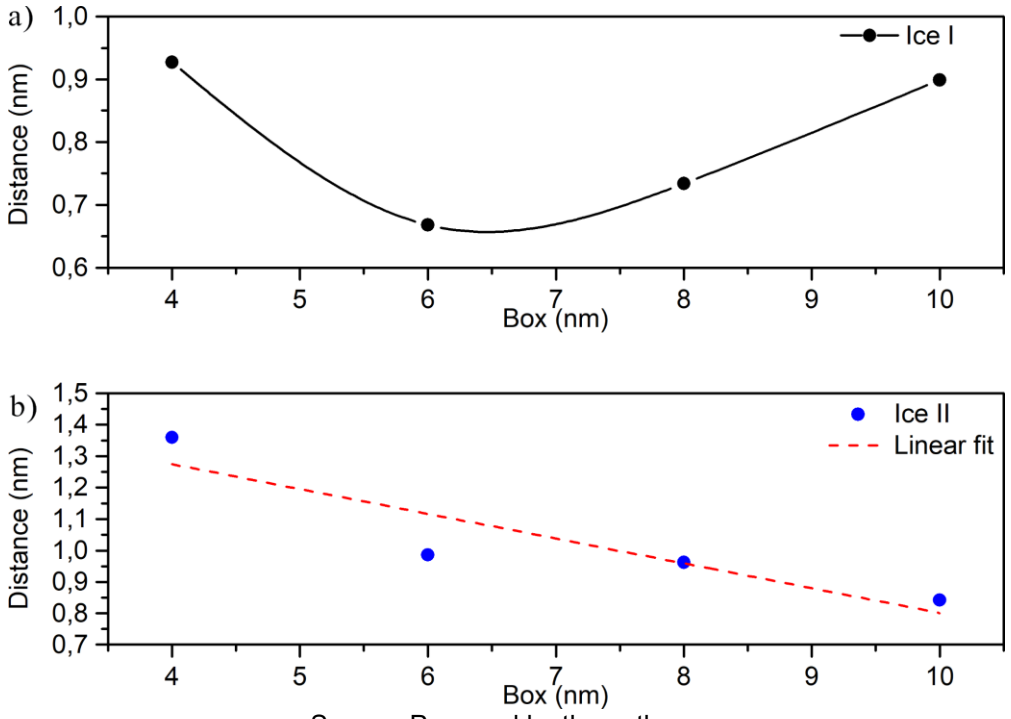

Source: Prepared by the authors.

We noticed that for system I there is an initial height of the simulation box, which causes the average distance of the molecules in relation to the graphene to increase as a function of the height of the box, during the process of ice formation adsorbed to the surface. System II presents a linear relationship between the average distance of the molecules and the graphene surface during the ice formation process, in such a way that we realize that the higher the initial height of the simulation box, the closer the molecules are adsorbed to the surface. Next section, we will discuss the observed phenomenon and its relationship with the hydrogen bonds.

3.4 HYDROGEN BONDS

In this work, we analyze the average number of hydrogen bonds, as a function of the initial height of the simulation box, generated at the end of the simulation when the astrophysical ice adsorbed to the graphene substrate is formed. The results are shown in figure 4.

Figure 4 presents the variation in the amount of the number of hydrogen bonds (NHB) for the studied ices depending on the initial height of the simulation box.

Figure 4 - Shows the variation in the number of total hydrogen bonds as a function of the initial height of the simulation box during the ice formation process I and II using the last frame of the simulation.

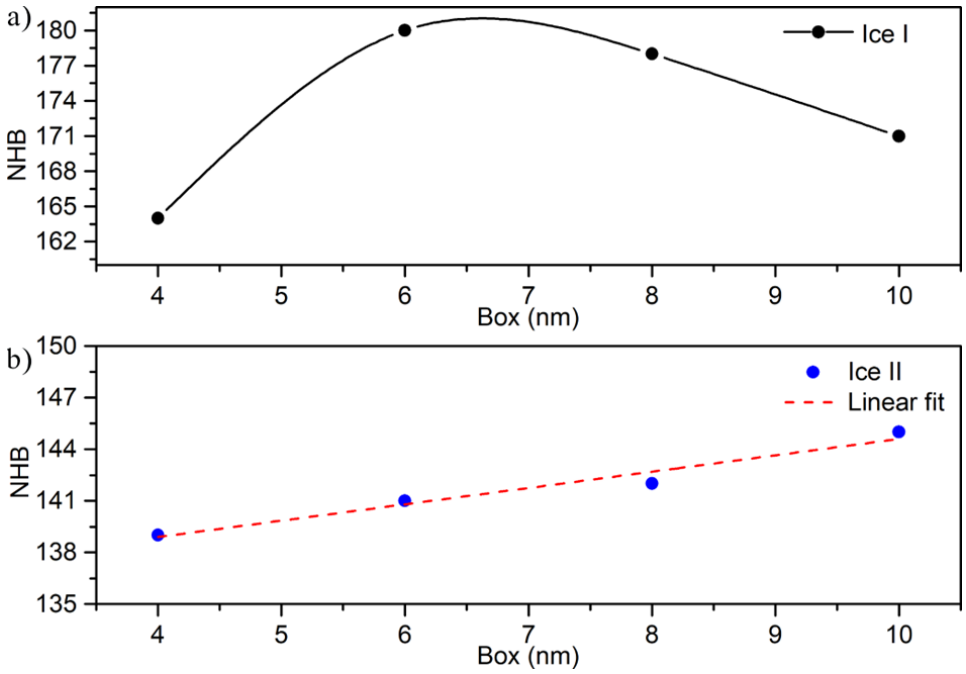

Source: Prepared by the authors.

For system I, we observed that when the simulation box was initially at a height of 4 nm the NHB referring to the last 1.0 ps of simulation was 164, for the height of 6 nm it increased to 180, then as the height of the box changed to 8 nm we obtained the value of 178 and finally for 10 nm the value of 172. As for the formation of ice adsorbed to graphene, starting from system II, we observed that when the box and simulation was at a height of 4 nm, the NHB was 139 in the last 1.0 ps, for 6 nm this number increased to 141, for the height of 8 nm 142 connections and for 10 nm we obtained the number of 145.In general, we noticed that system I, consisting only of molecules of H_2O and graphene, generated a higher number of hydrogen bonds at the end of the simulation, when compared to system II, consisting of H_2O, CO_2 and graphene. We observe that for system I there is a box height that provides a drop in the number of hydrogen bonds as a function of the initial increase in the box, while for system II, we notice that the greater the initial height of the simulation box, the greater the number of hydrogen bonds. Next, we present the method used to determine the density of an astrophysical ice nanostructure.

3.5 AVERAGE DENSITY OF ASTROPHYSICAL ICES

The astrophysical ice nanostructures adsorbed to the graphene surface present irregular patterns that are related to the initial configuration of the systems in the gas phase, chemical composition, and the initial height of the simulation box in the gas phase. The formed ice nanostructures present irregular patterns, as can be seen in Figures 5 and 6. Thus, to determine the density of the ices adsorbed on the graphene surface we delimit two volumes, the first with a radius three times the average of a hydrogen bond and the second with a radius twice that of a hydrogen bond. We considered a region that had a higher density of molecules and selected 5 molecules, which served as references to delimit the sphere radius. This procedure allowed us to obtain a volume average, and consequently a density average, for ice I and ice II formed from different average molecular heights related to the different heights of the simulation box. Table 1 presents the average values of density as a function of the initial height of the box for a radius of approximately 9 and 6 Å. Figure 7 shows the density variation as a function of the initial size of the box.

Figure 5 - Panel a) shows the formation of ice I starting from a 4 nm high simulation box, panel b) the ice formation starting from the height of 6 nm, panel c) starting from the height of 8 nm and panel d) system I starts from a height of 10 nm.

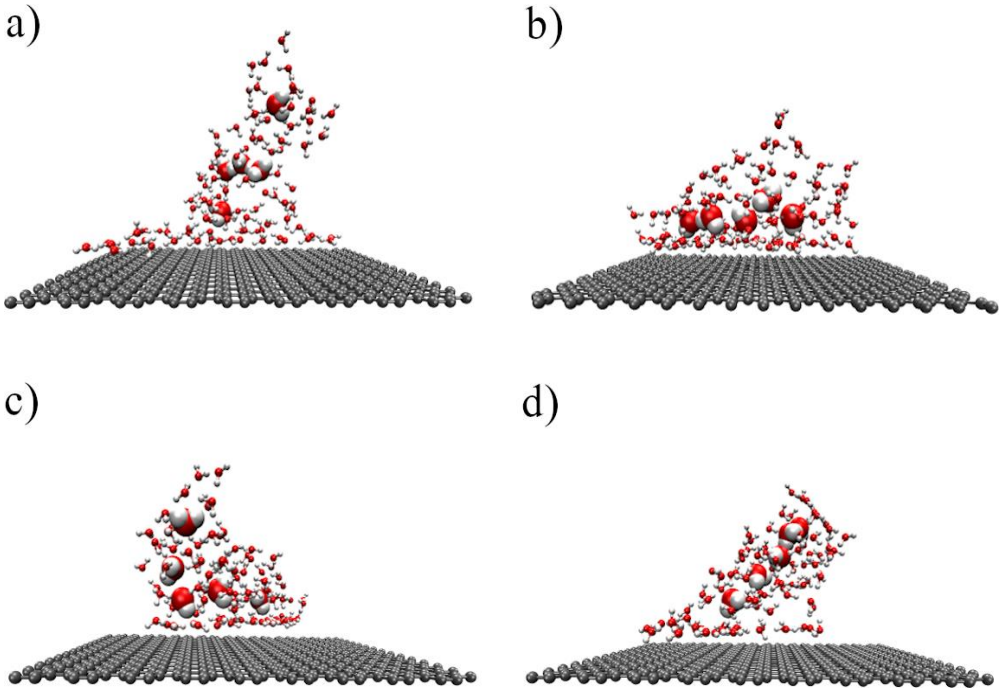

Source: Prepared by the authors.

Figure 6 - Shows the astrophysical ice formation starting from system II. Panel a) shows the formation of ice II starting from the initial height of 4 nm, panel b) starting from the height of 6 nm, panel c) starting from the height of 8 nm and panel d) starting from the initial height of 10 nm.

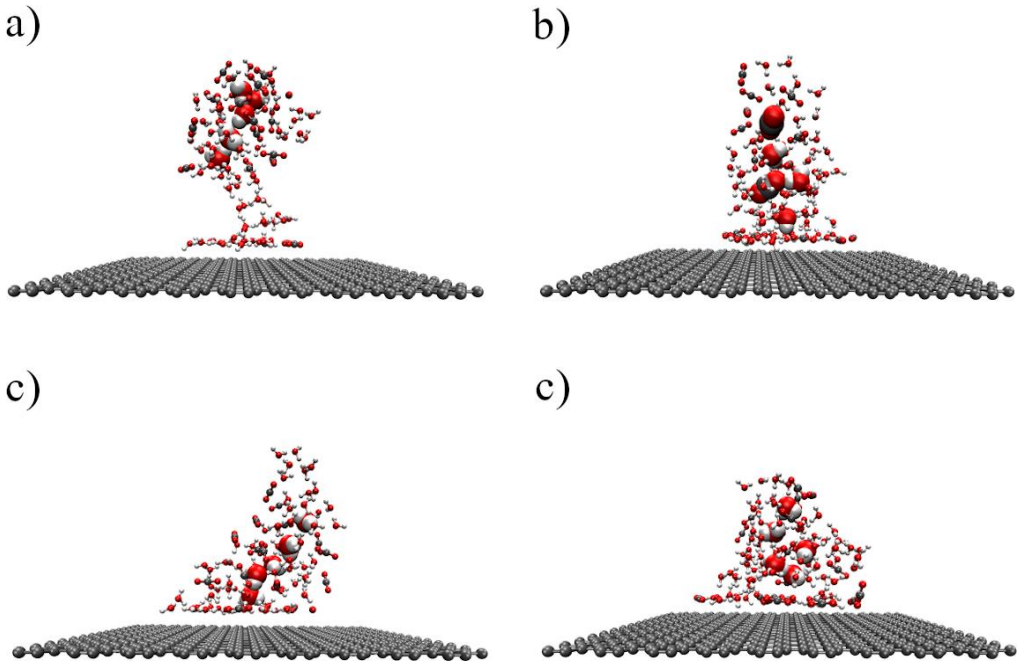

Source: Prepared by the authors.

Figures 5 and 6 highlight the molecules that were selected to delimit the 9 Å and 6 Å radii, that is, 3 and 2 times the size of an average hydrogen bond.

Table 1 - Mean density values for the astrophysical ices formed from System I and II as a function of the height of the box and for different radii.

Box initial height (nm)	Average density (g cm^{-3}) for a radius of 9 Å - Ice I	Average density (g cm^{-3}) for a radius of 6 Å - Ice I	Average density (g cm^{-3}) for a radius of 9 Å - Ice II	Average density (g cm^{-3}) for a radius of 6 Å - Ice II
4	0.411	0.664	0.397	0.521
6	0.392	0.542	0.379	0.492
8	0.337	0.482	0.454	0.574
10	0.333	0.469	0.290	0.538

Source: Prepared by the authors.

The determination of the density of astrophysical ice nanostructures based on the estimation of two cutting radii (9 and 6 Å), shown in Table 1 and used to define a volume and therefore measure the amount of molecules contained around a reference molecule, made us realize that the greater the radius, the lower the density, regardless of the type of ice analyzed. This fact may be related to the amorphous structure obtained, which does not present a homogeneous distribution, which in turn leads us to believe that by increasing the radius we considered more empty spaces than spaces with molecules.

Figure 7 - Shows the graph of the variation of the density of ice I (a) and ice II (b) as a function of the initial height of the simulation box.

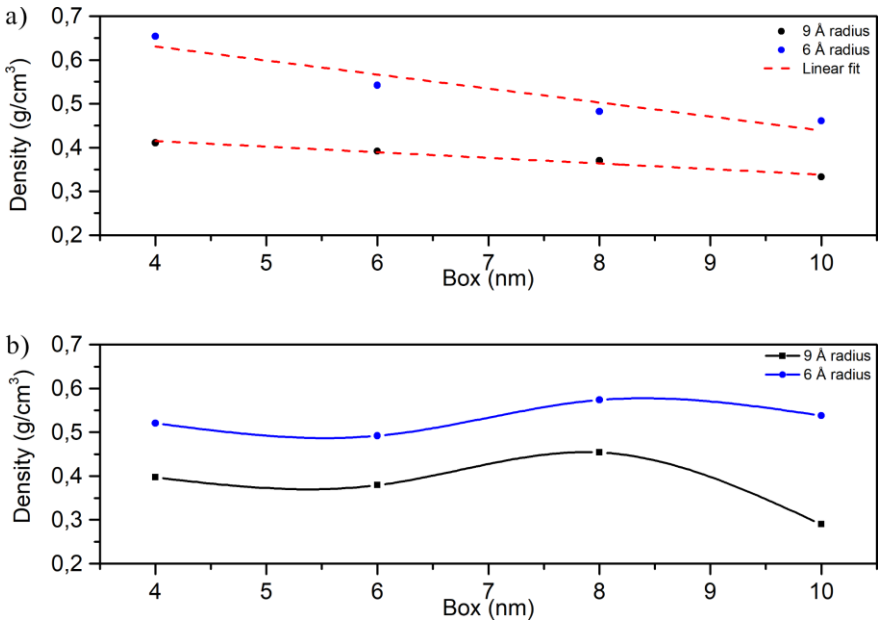

Source: Prepared by the authors.

The graph shown in figure 7 shows the variation in the average density of the ices adsorbed on the graphene surface, obtained after choosing 5 reference molecules that delimited the cut radii of 6 and 9 Å, as a function of the initial height of the simulation box. Figure 7a represents system I, forming ice I. We notice that the size of the box has an inversely proportional influence on obtaining average density, that is, when determining the density of amorphous ice formed in a 9 nm box, the molecules are away from the central reference molecule, which generates the formation of lower density ice. When we look at figure 7b, which represents ice II, we see an alternation between the increase and decrease in density as a function of the size of the box.

4 CONCLUSION

In this theoretical work employing molecular dynamics in the field of astrophysics and astrochemistry, we simulated nanostructures of astrophysical ices formed from a system with water and another with water and carbon dioxide, adsorbed to the graphene substrate at a temperature of 10 K. The formation of astrophysical ice via the MD technique was only possible when performing the procedure of opening the simulation box, in which the removal of the barostat from the system, a condition that allowed us to simulate the "vacuum", keeping the graphene substrate fixed in the lower part of the system frozen at 10 K. Our main results are summarized below:

i) Different initial configurations produce different ice nanostructures. This effect is observed both in the choice of initial conditions of the system, as in its homogeneity.

ii) There is a relationship between the average distance of the center of mass of the molecules of systems I and II in relation to the center of mass of graphene, when we observe this variation as a function of the initial size of the simulation box

and the number of hydrogen bonds. We noticed that the smaller the initial height of the simulation box, the greater the average distance from graphene and the smaller the number of hydrogen bonds, in the same way that the greater the initial size of the simulation box, the smaller the average distance of the molecules in the system and the greater the number of hydrogen bonds.

iii) The hydrogen bonds help in the process of stabilizing the molecular nanostructures of the astrophysical ices formed, in this way ice I (polar) has a greater stability than ice II (non-polar).

iv) The irregular shape of the nanostructures of the ice obtained makes it difficult to determine its density, however, by delimiting a radius around a molecule, we can estimate the mass and volume and, therefore, the density of the ice for each height, resulting in the fact that ice II has a lower average density than ice I, which in turn may be related to the low hydrogen bond that provides this system with greater mobility and greater volume. This theoretical study helps to better understand the formation of astrophysical ice nanostructures and the effects of nonpolar species (e.g., CO_2) within the ice and how this can influence the freezing process of ice in space. Future works will also describe, using MD, the desorption processes during the heating of these studied ice systems.

REFERENCES

Abraham, M. J., Van Der Spoel, D., Hess, B. & Lindahl, E. E. (2014). The GROMACS development team, *GROMACS User Manual* (version 4.6.7).

Anders, C. & Urbassek, H. M. (2013). Impacts into cosmic ice surfaces: A molecular-dynamics study using the Reax force field. *Nuclear Instruments and Methods in Physics Research Section B*, *303*, 200–204. https://doi.org/10.1016/j.nimb.2012.10.015

Andersson, S. & Van Dishoeck, E. F. (2008). Photodesorption of water ice. *Astronomy & Astrophysics*, *491*, 907–916. https://doi.org/10.1051/0004-6361:200810374

Andersson, S., Al-Halabi, A., Kroes, G.-J. & Van Dishoeck, E. F. (2006). Molecular-dynamics study of photodissociation of water in crystalline and amorphous ices. *The Journal of Chemical Physics*, *124*, 064715-1 - 064715-14. https://doi.org/10.1063/1.2162901

Arasa, C., Van Hemert, M. C., Van Dishoeck, E. F. & Kroes, G. J. (2013). Molecular Dynamics Simulations of $\boldsymbol{CO_2}$ Formation in Interstellar Ices. *The Journal of Physical Chemistry A*, *117*(32), 7064–7074.

Arasa, C., Andersson, S., Cuppen, H. M., van Dishoeck, E. F. & Kroes, G.-J. (2010). Molecular dynamics simulations of the ice temperature dependence of water ice photodesorption. *The Journal of Chemical Physics*, *132*, 184510-1 - 184510-12. https://doi.org/10.1063/1.3422213

Berendsen, H. J. C., Spoel, D. van der. & Drunen, R. van. (1995). GROMACS: A message-passing parallel molecular dynamics implementation. *Computer Physics Communications, 91*, 43–56.

DePaul, A. J., Thompson, E. J., Patel, S. S., Haldeman, K. & Sorin, E. J. (2010). Equilibrium conformational dynamics in an RNA tetraloop from massively parallel molecular dynamics. *Nucleic Acids Research*, *38,* 4856–4867. http://doi.org/10.1093/Nar/Gkq134

Ehrenfreund, P. & Charnley, S. B. (2000). Organic Molecules in the Interstellar Medium, Comets, and Meteorites: A Voyage from Dark Clouds to the Early Earth. *Annu. Rev. Astron. Astrophys*, *38,* 427–483. https://doi.org/10.1146/annurev.astro.38.1.427

Freivogel, P., Fulara, J. & Maier, J. P. (1994). Highly Unsaturated Hydrocarbons as Potential Carriers of Some Diffuse Interstellar Bands. *The Astrophysical Journal*, *431*, 151–154.

Gerakines, P. A., Whittet, D. C. B., Ehrenfreund, P., Boogert, A. C. A., Tielens, A. G. G. M., Schutte, W. A., Chiar, J. E., van Dishoeck, E. F., Prusti, T., Helmich, F. P. & de Graauw, Th. (1999). Observations of Solid Carbon Dioxide in Molecular Clouds with the Infrared Space Observatory. *The Astrophysical Journal*, *522*, 357–377. https://doi.org/10.1086/307611

Kwok, S. (2016). Complex organics in space from Solar System to distant galaxies. *The Astronomy and Astrophysics Review*, *24*(8), 1–27. https://doi.org/10.1007/s00159-016-0093-y

Mainitz M., Anders C. & Urbassek, H. M. (2016). Irradiation of astrophysical ice grains by cosmic-ray ions: a REAX simulation study. *Astronomy & Astrophysics*, *592*, A35–A45. https://doi.org/10.1051/0004-6361/201628525

Matsumoto, M., Saito, S. & Ohmine, I. (2002). Molecular dynamics simulation of the ice nucleation and growth process leading to water freezing. *Nature*, *416*, 409–413.

Rino, F. P., Costa, B. V. (1998). *ABC da simulação computacional* (1. ed.). Brasil.

Sorin, E. J. & Pande, V. S. (2005). Exploring the Helix-Coil Transition via All-Atom Equilibrium Ensemble Simulations. *Biophisical Journal*, *88*, 2472–2493. https://doi.org/10.1529/biophysj.104.051938

Tielens, A. G. G. M. (2005). *The Physics and Chemistry of the Interstellar Medium* (1. ed.). Cambridge University Press.

Tielens, A. G. G. M. (2013). The molecular universe. *Reviews of Modern Physics*, *85*, 1021–1081. https://doi.org/10.1103/RevModPhys.85.1021

Van Dishoeck, E.F. (2014). Astrochemistry of dust, ice and gas: introduction and overview. *Faraday Discussions*, *168*, 9–47. https://doi.org/10.1039/C4FD00140K

Zheligovskaya, E.A. (2008). Molecular dynamics study of crystalline water ices. *Journal of Structural Chemistry*, *49*, 459–471.

ACKNOWLEDGMENTS

The authors acknowledge the Fundação Valeparaibana de Ensino/Universidade do Vale do Paraíba (FVE-UNIVAP) and the Brazilian research agencies Conselho Nacional de Desenvolvimento Científico e Tecnológico - CNPq (#302608/2022-2; #304130/2012-5; 306145/2015-4; 302985/2018-2, 2535/2017-1 and 437182/2018-5), Fundação de Amparo à Pesquisa do Estado de São Paulo - FAPESP (# JP 2009/18304-0) and the Coordenação de Aperfeiçoamento de Pessoal de Nivel Superior - CAPES (Finance Code 001). RGA also acknowledges financial support from the FAPERJ under grant number E-26/010.101126/2018 and 26/202.699/2019. PAS thanks the Superintendência de Tecnologia da Informação of the Universidade de São Paulo (USP-Lorena) for the help with the utilization of the HPC resources.